International Journal of Mechanics and Energy (IJME)
Vol. 3, Issue 1, 2015, ISSN: 2286-5845

Half-metallic ferromagnetism in the Mn_2CoAs Heusler compound

Miloud Ibrir[1,*], Said Lakel[2], Safia Alleg[3], Rachid Bensalem[3]

[1]Laboratory of Physics of Materials and its Applications, *Department of Physics, Faculty of sciences, University of M'sila, Algeria.*

[2]*Laboratory of Metallic and Semiconducting Materials (LMSM) University of Biskra, Algeria.*

[3]*Department of Physics, Faculty of sciences, University of Annaba, Algeria.*

Abstract: First-principles calculations for the structural, electronic, and magnetic properties of Mn_2CoAs Heusler compound, have been performed for using full-potential linearized augmented plane wave (FP-LAPW) scheme within the (GGA-WC) and GGA+U. Features such as the lattice constant, bulk modulus, and its pressure derivative are reported, in addition to the results of the band structure and the density of states. The electronic structure in the ferromagnetic configuration for Mn_2CoAs Heusler compound shows that the spin-up electrons are metallic, but the spin-down bands have a gap of 0.48 and 0.77 eV for GGA-WC and GGA+U, respectivly. The Mn_2CoAs Heusler is ferrimagnetic and maintains the half-metallic character having 100 % polarization for lattice parametres in 5.5 and 5.82 Å.

Key words: Heusler compounds; FP-LAPW; DFT+U; Spintronics.

1. Introduction

Heusler compounds are ternary intermetallic compounds that have the general composition X_2YZ. In this class, X and Y represent d-electron transition metals, and Z denotes an sp-electron element [1]. In recent years, Heusler compounds have been extensively studied, and motivated by their gained importance due to advancements in spintronics [2–6]. In contrast to half- metallic ferromagnets (HMFs) [7], only a few Heusler compounds (all of them with a rare earth metal at the Y position) have been successfully implemented as superconductors [8]. Pd_2YSn is the Heusler compound with the highest critical temperature (4.9K) [9]. The coexistence of antiferromagnetism and superconductivity demonstrating the manifoldness of the Heusler family, was reported for Pd_2YbSn [10] and Pd_2ErSn [11].

*** Corresponding author:** Miloud Ibrir
E-mail: ibrirmiloud@yahoo.fr

Many of the Heusler compounds have been reported to be HMFs [12,13], and several Co_2-based Heusler compounds have been used as electrodes in magnetic tunnel junctions [14,15]. The hexagonal compound Pd_2CeIn orders antiferromagnetically at 1.23 K [16]. D. B. de Mooij et *al.*[17] reported that Pt_2GdSn and Pt_2ErSn exhibit ferromagnetic (Tc= 20 K) and paramagnetic behavior, respectively. Generally, Heusler compounds (X_2YZ) crystallize in the cubic L2*1* structure (spacegroup Fm3m), the X_2 atoms form a primitive cubic sublattice and adjacent cubes of this X_2 sublattice are filled by alternating Y or Z atoms. If the number of 3d electrons of Y atom is more than X atom, we can observe $CuHg_2Ti$-type structure with the space group F43m. In this structure, X atoms occupy the nonequivalent 4a(0,0,0) and 4c(1/4,1/4,1/4) positions, while Y and Z atoms are located at 4b(1/2,1/2,1/2) and 4d(3/4,3/4,3/4) positions, respectively [18].

In the present paper, the structural, electronic, and magnetic properties of Mn_2CoAs are reported. The aim of this work is to evaluate the validity of the predictions of half metallicity for Mn_2CoAs Heusler compound. The calculations are performed using ab-initio full-potential linearized augmented plane wave (FP-LAPW) within the density functional theory (DFT) with the generalized gradient approximation GGA-WC and GGA+*U*. In this paper, we organized the theoretical background as its showed in Section 2. The results and discussions are mentioned in Section 3. The summary of our results is given in Section 4.

2. Method of calculations

First principles calculations [19, 20] with both full potential and linear augmented plane wave (FP-LAPW) method [21] as implemented in the WIEN2k code [22] have been employed. The exchange-correlation effects were described with the parameterization of the generalized gradient approximation (GGA) by Wu and Cohen (GGA-WC) [23] and GGA+*U* [24]. In these calculations the parameter $R_{MT}K_{max}$=9, which determines matrix size (convergence), that is to say that K_{max} is the plane wave cut-off and R_{mt} is the smallest of all atomic sphere radii. The muffin-tin radii (MT) are for Mn, Co, and As to be 2.1, 2.2 and 2.25 (a.u), respectively. Within the spheres, the charge density and potential are expanded in terms of crystal harmonics up to angular momenta L=10 and a plane wave is used in the interstitial region. The value of G_{max}=14, where G_{max} is defined as the magnitude of largest vector in charge density Fourier expansion. The Monkorst-Pack special k-points were performed using 1500 special k-points in the Brillouin zone for Mn_2CoAs compound [25]. The cut off energy, which defines the separation of valence and core states, was chosen as -6 Ry. We select the charge convergence as 0.0001*e* during self-consistency cycles. In the GGA+*U* calculations, an effective parameter $U_{eff} = U - J$ has been used, where U is the Hubbard parameter and J *is* the exchange parameter. U and J are given the values of 7.07 and J = 0.0 eV, respectively.

3. Results and discussion

The total energy is calculated (Fig. 1) as a function of lattice constant of Mn_2CoAs compound for the ferromagnetic (FM) state. In order to determine the ground state properties, such as equilibrium lattice constant a, bulk modulus B and its pressure derivative B', the total energies versus changed volumes are fitted to the Murnaghan's equation of state [26]. The calculated structural parameters of Mn_2CoAs compound obtained in this work reported in Table 1 with these found in the literature are in good agreement with the theorical data of reference [27]. In our knowledge there are no experimental data or theoretical calculations exploring the bulk modulus and its pressure derivative for this compound. The bulk modulus and its pressure derivative B' data for Mn_2ZnSi [28] and Ti_2CoGa [29] are also presented in Table 1 for a direct comparison purpose.

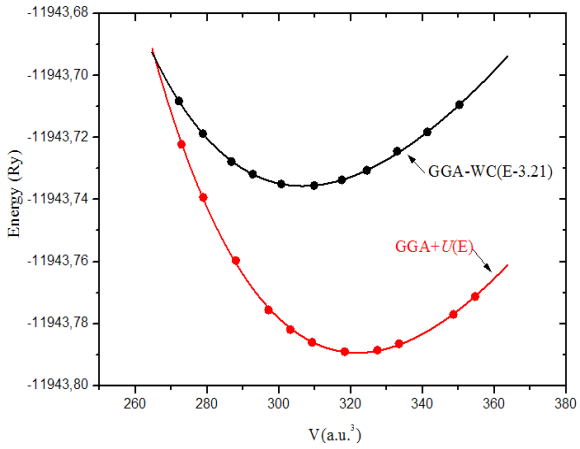

Fig. 1 Volume optimization for the Mn_2CoAs Heusler compound.

The calculated spin-polarized band structures of Mn_2CoAs compound at the theoretical equilibrium lattice constant along high-symmetry directions of the first Brillouin zone are displayed in Fig. 2. Note that, there is no difference in the band structure plot for the two approaches.

Table 1 Lattice constant a(Å), bulk modulus B (in GPa), pressure derivative of bulk modulus B', total and partial magnetic moment (in μB) for Mn2CoAs compound.

compound		(GGA-WC)	GGA+U	Previous [27]
Mn_2CoAs	a	5.68	5.76	5.74
	B	221.91	191.08	-
	B'	6.23	4.75	-
	$m_{Mn(1)}$	0.163	-0.008	-0.04
	$m_{Mn(2)}$	2.689	2.798	3.04
	m_{Co}	1.045	1.104	0.98
	m_{As}	0.016	0.041	0.02
	m_{Total}	3.978	4.002	4
Mn_2ZnSi [28]	B	138.665	-	-
	B'	4.525	-	-
Ti_2CoGa [29]	B	140.369	-	-
	B'	4.525	-	-

The total, atom-projected and partial densities of states, in which the spin-up and spin-down sub-bands are plotted with black and red lines, respectively, as shown in Figs. 2–4. The Fermi level set as 0 eV.

In Fig. 2, the spin-up band structure has apparently a metallic intersections at the Fermi level, indicating a strong metallic nature of the spin-up electrons. In minority-spin band, the valence band maximum (VBM) is located at point Γ, where as the conduction band minimum (CBM) is located at Γ point, leads to a gap of about 0.48 and 0.77 eV for GGA-WC and GGA+U, respectivly. The spin-down band structure exhibits a band gap indicating semiconducting nature at the Fermi level. This energy gap in the minority-spin band gap leads to 100% spin polarization at the Fermi level. Therefore, the result reveals that Mn_2CoAs compound exhibits half-metallic properties.

In Fig. 3 shows the total density of states and atom-projected (TDOS) as a function of energy for the Mn_2CoAs compound at its equilibrium lattice constant. To illustrate the nature of the electronic band structures, we plotted the partial density of states (DOS) of Mn(1)-3d, Mn(2)-3d, Co-3d and As-p

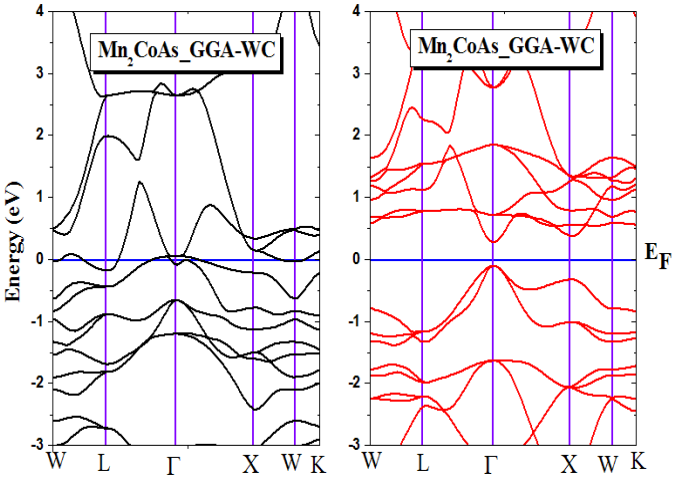

Fig. 2 Up- and down-spin Band structures for Mn2CoAs compound along the high symmetry axes of the Brillouin Zone.

electrons for the spin-up and spin-down sub-bands in Fig. 4. The figure indicates that band structures can be divided into two parts: at the energie rigon from –9.0 to –4.0 eV we find the contribution of As-p electrons, but the energie rigon -4.0 to 4.0 eV reprsents the contribution of the Mn(1)-3d and Mn(2)-3d state hybridized with Co-3d orbital.

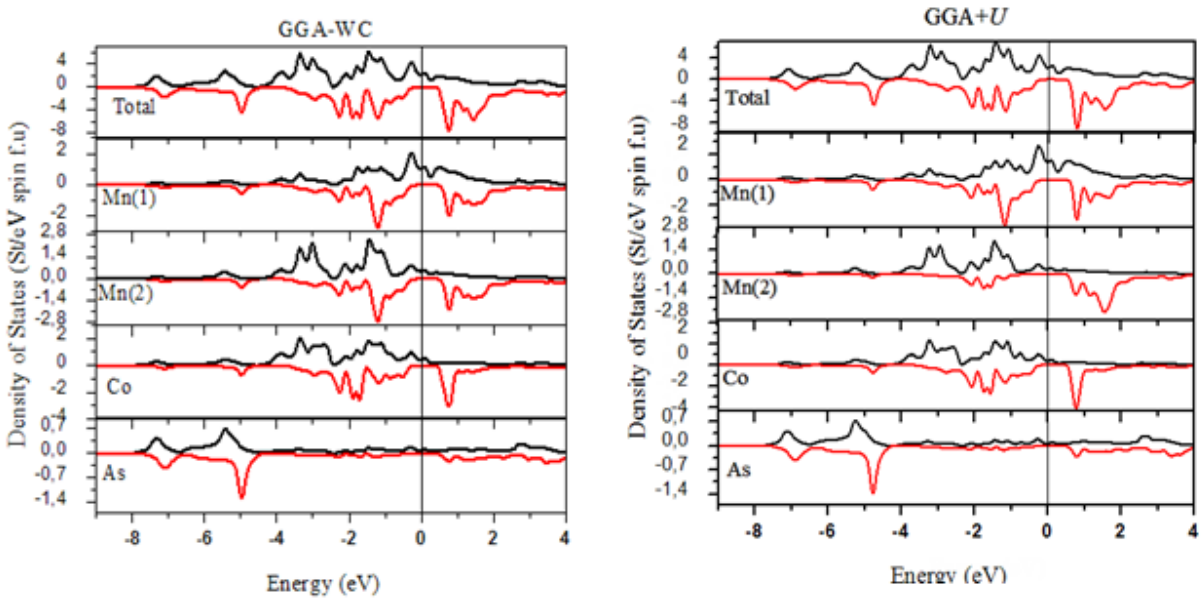

Fig. 3 The total density of states (TDOS) and atom-projected DOS.

The results of the calculated total and atom-resolved magnetic moments, using GGA-WC and GGA+*U* of Mn_2CoAs compound, are summarized in Table 1. The present study shows that the total magnetic moment of Mn_2CoAs compound are 3.97 to 4.00 μ_B for GGA-WC and GGA+*U*, respectivly. These results are in good agreement with previous theorical work [27]. The obtained result with the GGA+*U* method is in better agreement with the theorical data compared to those calculated by the GGA-WC method. The using of the *U*-Hubbard term, decreased the magnetic moment significantly. For Mn_2CoAs Heusler compound, the magnetic moments come from the exchange-splitting of the 3d states of the Mn(1), Mn(2) and Co ions. Furthermore, for this compound the partial moment of As atom is the smallest, so its contribution in the total magnetic moment.

In Table 2 showed a detailed information on the atomic and total magnetic moments and the spin polarization as a function of lattice constant, where the total magnetic moment vary from 4.00 to 3.98 μ_B. The calculated magnetic moments of the Mn(2) and Co atoms increase with the increase of the lattice parameter, while the magnetic moment of the Mn(1) atom decreases. In order to investigate the dependence of the half-metallic state on the lattice parameter, calculations have been performed for the lattice parameters between 5.5 and 5.82 Å. Fig.5 shows cleary that the Mn_2CoAs Heusler compound has half-metallic nature above the lattice constant values of 5.82 Å. Therefore, the lattice constant variation does not affect half-metallic behavior of the Mn_2CoAs compound.

4. Conclusion

Here, using the FP-LAPW methods implemented in the Wien2k within GGA-WC and GGA+*U*. The original aspects of the present calculations concern the structural, electronic and magnetic properties of Mn_2CoAs Heusler compound. The electronic structure in the ferromagnetic configuration for Mn_2CoAs Heusler compound show that the spin-up electrons are metallic, but the spin-down bands have a gap of 0.48 and 0.77 eV for GGA-WC and GGA+*U* respectivly. the magnetic moments were mostly contributed by the

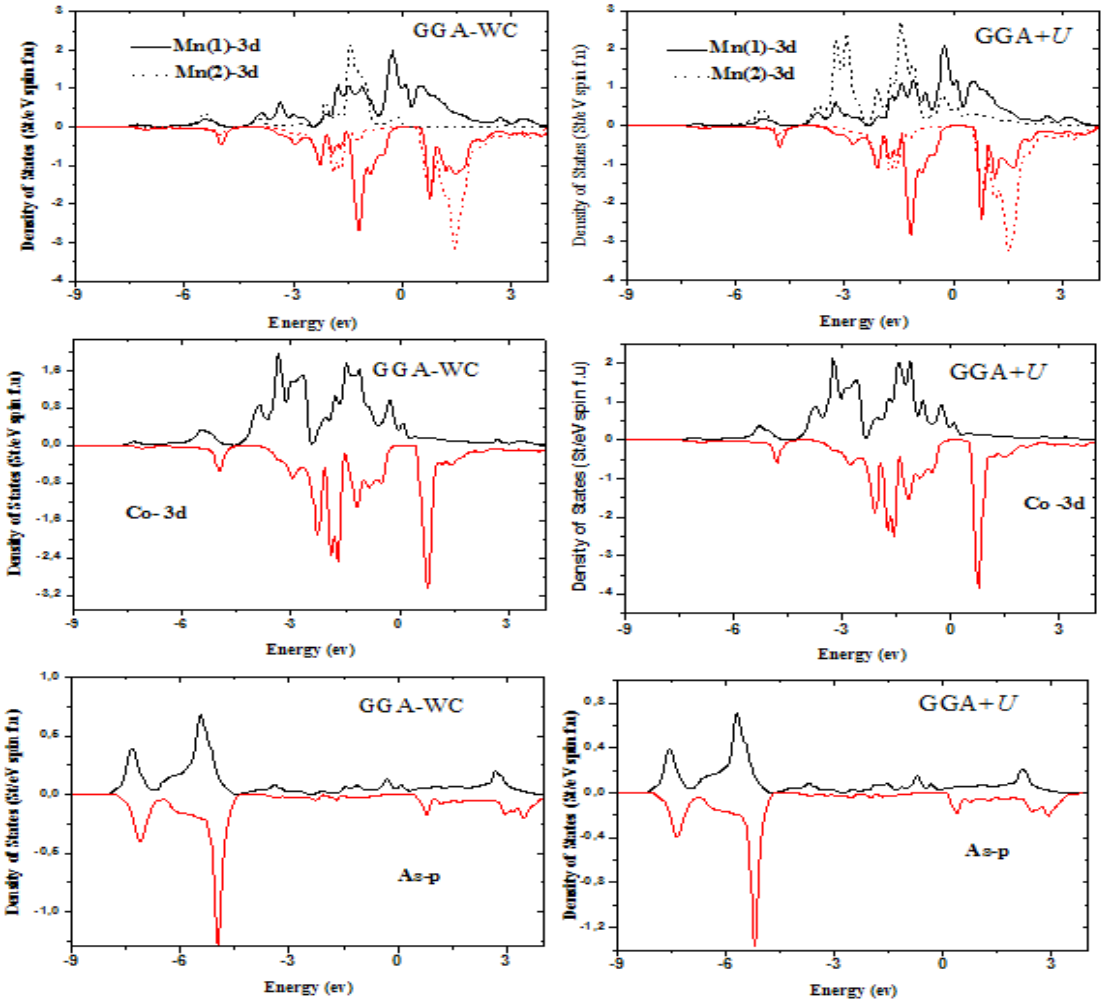

Fig. 4 Spin polarized partial DOS of Mn2CoAs compound.

Table 2 Calculated spin polarization, total and atom-projected magnetic moments as a function of the lattice parameter.

Method	a (Å)	Mn(1)	Mn(2)	Co	Spin polarization ratio (%)	Total magnetic moment
GGA-WC	5.50	0.181	2.667	1.012	100	4.002
	5.58	0.152	2.673	1.041	100	4.001
	5.74	0.111	2.718	1.052	100	4.001
	5.83	-0.025	2.815	1.082	97	3.999
	5.93	-0.205	2.926	1.129	92	3.982
GGA+*U*	5.49	0.219	2.641	1.011	100	4.002
	5.60	0.201	2.649	1.041	100	4.000
	5.68	0.124	2.707	1.065	100	4.000
	5.82	-0.057	2.839	1.104	97	3.999
	5.95	-0.352	3.017	1.194	92	3.980

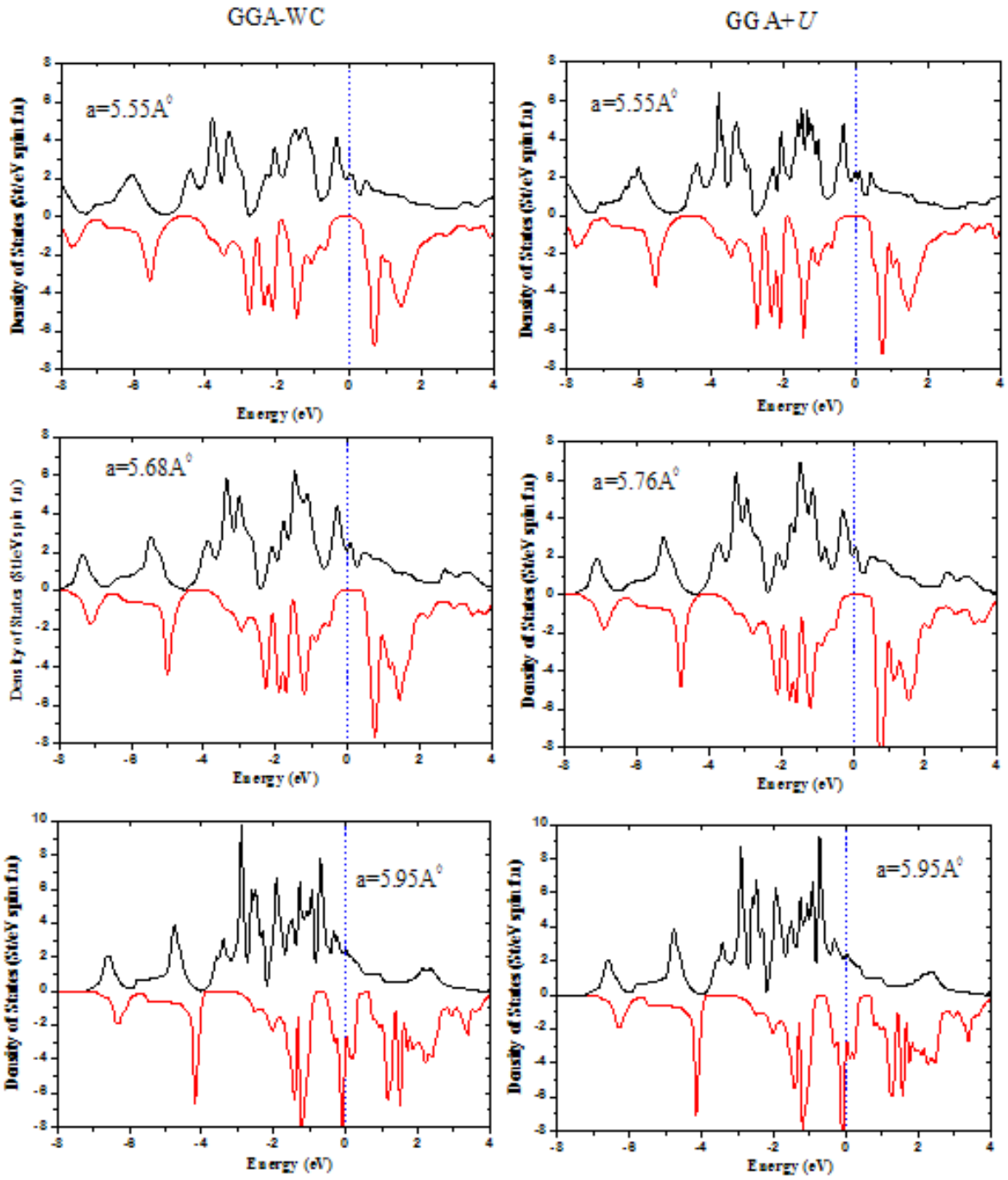

Fig. 5 Total TDOS for the Mn_2CoAs alloy as a function of the lattice constant. Black color (positive value) corresponds to spin-up and red color (negative value) line spin-down electrons.

3d orbital of Mn(1), Mn(2) and Co ion. Our calculations show that Mn_2CoAs Heusler compound is candidate material for future spintronic applications.

Références

[1] P.J.Webster; J. Phy. Chem. Soli. **32** (1971) 1221–1231

[2] S.A. Wolf, D.D. Awschalom, R.A. Buhrman, J.M. Daughton, S. Von Molnar, M.L. Roukes, A.Y. Chtchelkanova and D.M. Treger; Science **294** (2001) 1488-1495

[3] G.A. Prinz; Science **282** (1998) 1660-1663

[4] Y. Ohno, D.K. Young, B. Beshoten, F. Matsukura, H. Ohno, and D.D. Awschalom; Nature **402** (1999) 790-792.

[5] T. Dietl, H. Ohno, F. Matsukura, J. Cibert, and D. Ferrand; Science **287** (2000) 1019-1022.

[6] J.H. Park, E. Voscovo, H.J. Kim, C. Kwon, R. Ramesh and T. Venkatesh ; Nature **392** (1998) 794-796.

[7] R.A. de Groot, F.M. Mueller, P.G. van Engen and K.H.J. Buschow; Phys. Rev. Lett. **50** (1983) 2024-2027.

[8] M. Ishikawa, J.L. Jorda, and A. Junod; Superconductivity in d- and f-band metals; W. Buckel and W. Weber, Kernforschungszentrum Karlsruhe, Germany (1982).

[9] J.H. Wernick, G.W. Hull, T.H. Geballe, J.E. Bernardini and J.V. Waszczak; Mater. Lett. **2** (1983) 90-92.

[10] H.A. Kierstead, B.D. Dunlap, S.K. Malik, A.M. Umarji, and G.K. Shenoy; Phys. Rev. B **32** (1985) 135-138.

[11] R.N. Shelton, L.S. Hausermann-Berg, M.J. Johnson, P. Klavins, and H.D. Yang; Phys. Rev. B **34** (1986) 199-202.

[12] H.C. Kandpal, G.H. Fecher, and C. Felser; J. Phys. D: Appl. Phys. **40** (2007) 1507-1523.

[13] C. Felser, G. H. Fecher, and B. Balke. Angew. Chem. Int. Ed., **46** (2007) 668-699.

[14] T. Marukame, T. Ishikawa, S. Hakamata, K. Matsuda, T. Uemura and M. Yamamoto; Appl. Phys. Lett. **90** (2007) 012508-012510.

[15] N. Tezuka, N. Ikeda, S. Sugimoto and K. Inomata; Appl. Phys. Lett. **89** (2006) 252508-252510

[16] A.D. Bianchi, E. Felder, A. Schilling, M.A. Chernikov, F. Hulliger and H.R. Ott; Z. Phys. B **99** (1995) 69-72.

[17] D.B. de Mooij and K.H.J. Buschow; J. Less-Comm. Met. **102** (1984) 113-117.

[18] H.C. Kandpal, G.H. Fecher, C. Felser, J. Phys. D: Appl. Phys. **40** (2007) 1507.

[19] P. Hohenberg, W. Kohn; Phys. Rev. B **136** (1964) 864-871.

[20] W. Kohn, L.J. Sham; Phys. Rev. A **140** (1965) 1133-1138.

[21] J.C. Slater; Adv. Quant. Chem. **1** (1964) 5564.

[22] P. Blaha, Schwarz K., G.K.H. Madsen, D. Kvasnicka and J. Luitz, WIEN2K, an Augmented Plane Wave +Local orbitals program for calculating crystal properties (Karlheinz Schwarz, Technische Universität, Wien, Austria, 2001), ISBN 3-9501031-1-2.

[23] Z. Wu and R.E. Cohen; Phys. Rev. B **73** (2006) 235116-235121

[24] C. Loschen, J. Carrasco, K.M. Neyman and F. Illas, Phys. Rev. B **75** (2007) 035115-035122.

[25] H.J. Monkhorst and J.D. Pack; Phys. Rev. B **13** (1976) 5188-5192.

[26] F. D. Murnaghan; Proc. Natl. Acad. Sci USA **30** (1944) 244-247.

[27] S. Skaftouros, K. Özdoğan, E. Şaşıoğlu, I. Galanakis; arXiv:1002.3895 (unpublished).

[28] S. Kervan, N. Kervan ; Current Applied Physics **13** (2013) 80-83.

[29] N. Kervan, S. Kervan ; J. Magn. Magn. Mater **324** (2012) 645–648.